

## References

- BOEYENS, J. C. A. (1977). *Acta Cryst.* **A33**, 863–864.  
 BOEYENS, J. C. A. (1978). *J. Cryst. Mol. Struct.* **8**(6), 317–320.  
 DUAX, W. L. & NORTON, D. A. (1975). *Atlas of Steroid Structure*, Vol. 1, p. 16. New York: IFI/Plenum Data Co.  
 GERMAIN, G., MAIN, P. & WOOLFSON, M. M. (1971). *Acta Cryst.* **A27**, 368–376.  
 KAMANO, Y., PETTIT, G. R., INOUE, M., TOZAWA, M. & KOMEICHI, Y. (1977). *J. Chem. Res.* (**M**), 0837–0845.  
 MEINWALD, J., WIEMER, D. F. & EISNER, T. (1979). *J. Am. Chem. Soc.* **101**, 3055–3060.  
 ODE, R. H., PETTIT, G. R. & KAMANO, Y. (1975). *Cardenolides and Bufadienolides*, Vol. 8, edited by W. F. JOHNS, pp. 145–171. London: Butterworths.  
 SHELDRIK, G. M. (1978). *Computing in Crystallography*, edited by H. SCHENK, R. OLTHOF-HAZEKAMP, H. VAN KONINGSVELD & G. C. BASSI, pp. 34–42. Delft Univ. Press.

*Acta Cryst.* (1982). **B38**, 2166–2171

## Molecular Force-Field and X-ray Crystal Structures of Campanulin, a Comparison

BY FRODE MO

*Institutt for røntgenteknikk, Universitetet i Trondheim-NTH, N-7034 Trondheim-NTH, Norway*

(Received 28 September 1981; accepted 25 January 1982)

### Abstract

Molecular-mechanics calculations of campanulin, an 81-atom pentacyclic triterpenoid oxide, yielded structure parameters in generally good agreement with experimental values from a crystallographic study [Mo (1977). *Acta Cryst.* **B33**, 641–649]. The r.m.s. deviations between calculated and observed bond lengths, valency angles and torsion angles are 0.009 Å, 1.1° and 2°, respectively. Comparison with the corresponding experimental torsion angles in a closely related molecule indicates that some of these parameters in campanulin may be appreciably influenced by crystal forces. The calculated molecular geometry is very similar to that obtained in another study based on a significantly different force field [Faber (1977). Private communication]. The results demonstrate the ability of force-field methods to refine quite accurately the geometry of strained polycyclic systems of such complexity. Two different minimum-energy conformations of the molecule have been explored. Both calculations favour that found in the crystal by an energy difference of 7.7–12.4 kJ mol<sup>-1</sup> (1.85–2.95 kcal mol<sup>-1</sup>).

### Introduction

Molecular force-field (FF) calculations are being used increasingly as a method to evaluate for known molecules properties of both static and dynamic nature,

*e.g.* geometry, energies, heat of formation, vibrational frequencies *etc.*, and to predict such properties for related classes of unknown molecules (Engler, Andose & Schleyer, 1973; Altona & Faber, 1974; Dunitz & Bürgi, 1975; Ermer, 1976). Several force fields have been parametrized with respect to data obtained from diffraction, spectroscopy and thermochemical measurements and applied on a multitude of relatively simple molecules, mainly hydrocarbons. Extensive bibliographic lists of areas for FF studies are given by Engler *et al.* (1973) and Altona & Faber (1974). Apparently, total-valence FF investigations of more complex systems are rather few, one notable exception being a comprehensive study of steroid structures by Romers, Altona, Jacobs & de Graaff (1974); Altona & Faber (1974) discuss some other examples.

Fused hydrocarbon ring systems constitute an interesting group of compounds for FF calculations. The high internal strain that usually characterizes these molecules is reflected in large local variations in the structure parameters that will put the predictive abilities of any force field to test. Previous crystallographic studies of two related triterpenoids, baccharis oxide (Mo, 1973) and campanulin (Mo, 1977), led to the conclusion that their ring structures are considerably strained, largely due to a number of 1,3-diaxial methyl groups. Close agreement in geometry of the common structure fragments of the two compounds suggested that intermolecular forces play a minor role in determining the molecular conformation.

Campanulin (III and Fig. 1) is related to the

triterpene friedelane. An interesting aspect of this pentacyclic system pertains to the conformation of rings *D* and *E*. From inspection of molecular ball-and-stick (Dreiding) models Masaki, Niwa & Kikuchi (1975) described eight possible conformations for the *D/E cis*-fused rings of friedelane provided rings *A* to *C* are retained in the chair form. The latter condition is not met in campanulin, where the ether bridge between C(3) and C(10) has forced ring *A* to be boat and *B* twist-boat. These changes are remote from the rings of interest, however, and do not affect the arguments of Masaki *et al.* They concluded that the energetically favoured conformations are: (1) both rings *D* and *E* boat with C atoms 13,16 and 19,22 at bow and stern, which they called the stretched (*S*) form (I), and (2) both *D* and *E* deformed chairs = folded (*F*) form (II), energies increasing in that order. They observed the *S* form in crystals of 3 $\beta$ -*O*-acetyl-16 $\beta$ -*O*-(*p*-bromobenzoyl)pachysandiol B, which has a large substituent in  $\beta$  at C(16) (IVa). The *S* form was also found in 2,2-dibromo-27,28-epoxyfriedelane-1,3-dione featuring an O bridge between C(27) and C(28) (V, campanulin numbering as in Fig. 1) (Rogers, Williams, Joshi, Kamat & Viswanathan, 1974) and later in 3 $\beta$ -friedelanol (IVb) (Laing, Burke-Laing, Bartho & Weeks, 1977). On the other hand, an early two-dimensional X-ray study of 3 $\alpha$ -friedelanol chloroacetate, the 3 $\alpha$  epimer, had suggested that rings *D* and *E* are chairs (Corey & Ursprung, 1956), *i.e.* the conformation is *F* as in the crystal structure of (III). Laing *et al.* conclude from Dreiding modelling that the close 1,3 methyl contact C(24)···C(26) (campanulin numbering) in the *F* form prohibits its existence, and therefore the *D/E* rings of the friedelane skeleton will be in the *S* form. The results obtained for (III) and possibly also for the 3 $\alpha$ -friedelanol derivative are clearly at variance with this statement.

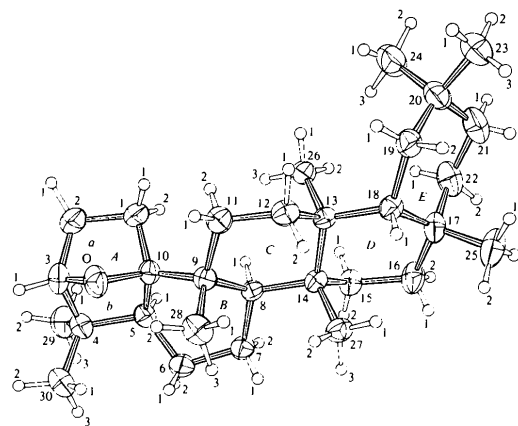
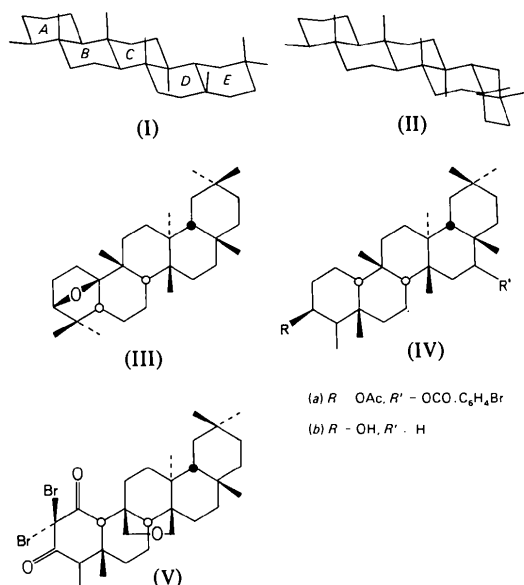


Fig. 1. Perspective view of campanulin showing atomic numbering and the labelling of the rings.

Molecular FF calculations provide a better tool for analysis of this conformational problem. Campanulin was chosen as the test case for several reasons: its crystal structure has been determined with good precision, errors in bond lengths and angles being about 0.004 Å and 0.2°, respectively; the molecular packing in the crystal is relatively loose, involving no short intermolecular van der Waals contacts and no hydrogen bonds; and comparison with the baccharis oxide structure provides a measure of the experimental accuracy, in particular of bond lengths and angles, in the common *a,b,A,B,C* ring fragment (Fig. 1).

### Calculations

FF calculations of structure and potential energy for both forms *F* and *S* of campanulin were carried out with a locally modified version of the program *MOLBD2* (Boyd, 1968; Boyd, Breiting & Mansfield, 1973). Starting coordinates for the *F* form were based on the crystal structure (Mo, 1977); the *S* form was constructed from the former.

The force field used was basically that of Boyd (Chang, McNally, Shary-Tehrany, Hickey & Boyd, 1970), for which there appear to be no published experimental parameters for ether O. Since this atom is located well away from the *D* and *E* rings, we chose to treat it as a tetrahedral C atom in the calculations, except that a reference value of 1.442 Å was used for the C—O bond. In the course of the work, a few parameters involving C were changed slightly; a systematic optimization of all FF constants was not attempted, however. Potential functions and constants used in the final calculations are listed in Table 1; values different from those of Chang *et al.* (1970) have been marked. Boyd (1975) has proposed that the original value of  $K_{\phi}$  for a C( $sp^3$ )—C( $sp^3$ ) single bond

should be increased by 20% corresponding to a torsional barrier of 2.5 kcal mol<sup>-1</sup> (10.47 kJ mol<sup>-1</sup>). In the present work the value 2.65 kcal mol<sup>-1</sup> (11.10 kJ mol<sup>-1</sup>) for  $K_\phi$  appeared slightly better. Calculation of torsional energy included all possible sequences  $X-C-(C,O)-Y$  about the C-C and C-O bonds, making altogether nine terms for each  $C(sp^3)-C(sp^3)$  and three for each  $C(sp^3)-O$  bond. The corresponding FF constants were then  $\frac{1}{2}$  and  $\frac{1}{3}$ , respectively, of the value for  $K_\phi$  in Table 1. This procedure, which is employed in Ermer & Lifson's (1973) scheme, was essential to obtain good agreement with observed torsion angles of this strained ring system. The reference value for a C-C<sub>qt</sub>-C valency angle (C<sub>qt</sub> = quaternary tetrahedral carbon) was changed to 109.5°, consistent with the

averaged experimental value. Further, reference values for the C<sub>t</sub>-C<sub>t</sub> and C<sub>t</sub>-O bonds (C<sub>t</sub> = tetrahedral carbon) were optimized; the present value for C<sub>t</sub>-C<sub>t</sub> is in good agreement with those of Ermer & Lifson (1973) and White & Bovill (1977).

Iterative minimization of the potential energy was terminated when the final r.m.s. shifts of the coordinates were ~0.001 and ~0.006 Å for forms *F* and *S*, respectively. Convergence of the *S* form was considerably slower, possibly indicating that this form does not have a well defined minimum-energy conformation. An 8 Å cut-off limit was used for the non-bonded interactions (NBI), giving nearly 2300 NBI's and a total of about 2880 terms for this 81-atom molecule. The calculated structure parameters for the *F* form are summarized in Tables 2, 3 and 4 under the entry B/M.\*

Table 1. Parameters for force-field calculations

The parameters are essentially those of Boyd (Chang, McNally, Shary-Tehrany, Hickey & Boyd, 1970). Modified or new terms and constants are marked with an asterisk. Molecular energies are in units of 10<sup>-11</sup> ergs molecule<sup>-1</sup>, distances in Å and angles in radians. Conversion factors to kcal mol<sup>-1</sup> or kJ mol<sup>-1</sup> (SI system) are 143.845 × 10<sup>11</sup> and 602.25 × 10<sup>11</sup>, respectively. C<sub>t</sub> = tetrahedral carbon, C<sub>qt</sub> = quaternary tetrahedral carbon.

$$V_{\text{tot}} = V(b) + V(\theta) + V(\phi) + V(r_{nb})$$

(a) Bond stretch;  $V(b) = \frac{1}{2} \sum K_b(b - b_r)^2$

|  | $K_b$ | $b_r$ (Å) |
|--|-------|-----------|
| C <sub>t</sub> -C <sub>t</sub>           | 4.40  | 1.521*    |
| C <sub>t</sub> -O*                       | 4.40* | 1.442*    |
| C <sub>t</sub> -H                        | 4.55  | 1.09      |
| C <sub>t</sub> -H (in -CH <sub>3</sub> ) | 4.70  | 1.09      |

(b) Bond bend;  $V(\theta) = \frac{1}{2} \sum K_\theta(\theta - \theta_0)^2$

|   | $K_\theta$ | $\theta_0$ (°)† |
|---|------------|-----------------|
| C-C <sub>t</sub> -C }<br>O-C <sub>t</sub> -C* }               | 0.800      | 111.0           |
| C-C <sub>qt</sub> -C }*<br>O-C <sub>qt</sub> -C }<br>C-O-C }  | 0.800      | 109.5*          |
| C <sub>t</sub> -C <sub>t</sub> -H }<br>O-C <sub>t</sub> -H* } | 0.608      | 109.5           |
| H-C <sub>t</sub> -H   | 0.508      | 107.9           |

(c) Torsion;  $V(\phi) = \frac{1}{2} \sum K_\phi(1 + \cos 3\phi)$

|  | $K_\phi$ | $\phi_0$ (°)† |
|--|----------|---------------|
| X-C <sub>t</sub> -C <sub>t</sub> -Y }*‡<br>X-O-C <sub>t</sub> -Y } | 0.01842* | 60            |

(d) Nonbonded interactions;  $V(r_{nb}) = \sum A[\exp(-Br)] - C/r^6$

|  | A     | B     | C    |
|--|-------|-------|------|
| C <sub>t</sub> ...C <sub>t</sub> }<br>C <sub>t</sub> ...O* } | 104.0 | 3.09  | 4.45 |
| C <sub>t</sub> ...H }<br>O...H* }                            | 30.0  | 3.415 | 0.96 |
| H...H  | 18.4  | 3.74  | 0.19 |

† Angles in degrees to be converted to radians for use.

‡ X, Y = C, O, H; i.e. a total of nine terms per C<sub>t</sub>-C<sub>t</sub> bond, three terms per C<sub>t</sub>-O bond. For use of  $K_\phi$ , see text.

## Results and discussion

Boyd's force field is a relatively simple one in the sense that it includes only two harmonic (bond stretch and angle bend) and two anharmonic energy terms (torsion and nonbonded interactions) for saturated hydrocarbon systems. A more elaborate force field devised by Ermer & Lifson (1973) includes, in addition, a number of cross terms of the types stretch-stretch, stretch-bend, etc. These terms are introduced primarily to improve calculations of vibrational data, but were also found to influence structure parameters significantly in some strained polycyclic hydrocarbons (Ermer, 1976). Faber (1977) has performed calculations of campanulin with this force field modified to accommodate O. His results are given in Tables 2-4 (entry EL/F) for comparative purposes, together with relevant observed parameters for baccharis oxide. The two sets of calculated structure parameters in the ether O region demonstrate the similarity of the two force fields in reproducing the X-ray result, including the O parameters.

Both force fields reproduce bond lengths about equally well, r.m.s. deviations from the experimental O-C and C-C values being 0.009 and 0.010 Å with B/M and EL/F, respectively (Table 2). For the common structure fragment EL/F predicts bond lengths with better accuracy; the difference between the two fields in this region is mainly due to lack of detail on the part of B/M in reproducing the large bond-length variations at C(5). However, the latter field gives about the same agreement with observations in all parts of the molecule, whereas EL/F calculates the 13 non-cor-

\* A list of calculated coordinates for the *F* form has been deposited with the British Library Lending Division as Supplementary Publication No. SUP 36760 (3 pp.). Copies may be obtained through The Executive Secretary, International Union of Crystallography, 5 Abbey Square, Chester CH1 2HU, England.

Table 2. Observed and calculated bond lengths (Å)

Calculated values under the entries B/M and EL/F are from the present work and after Faber (1977), respectively. Experimental values of some relevant bond lengths in baccharis oxide (Mo, 1973) are included.

|       | Campanulin (CA) |       |      |       | Baccharis oxide (BO) | $10^3 \times (CA_{obs} - BO_{obs})$ |     |
|-------|-----------------|-------|------|-------|----------------------|-------------------------------------|-----|
|       | B/M             |       | EL/F |       |                      |                                     |     |
|       | obs.            | calc. | obs. | calc. |                      |                                     |     |
| O-3   | 1.443           | 1.446 | +3   | 1.444 | +1                   | 1.448                               | -5  |
| O-10  | 1.454           | 1.452 | -2   | 1.447 | -7                   | 1.459                               | -5  |
| 1-2   | 1.546           | 1.546 | 0    | 1.548 | +2                   | 1.550                               | -4  |
| 1-10  | 1.539           | 1.543 | +4   | 1.547 | +8                   | 1.537                               | +2  |
| 2-3   | 1.533           | 1.528 | -5   | 1.524 | -9                   | 1.515                               | +18 |
| 3-4   | 1.543           | 1.536 | -7   | 1.533 | -10                  | 1.539                               | +4  |
| 4-5   | 1.564           | 1.542 | -22  | 1.563 | -1                   | 1.568                               | -4  |
| 5-6   | 1.511           | 1.528 | +17  | 1.512 | +1                   | 1.511                               | 0   |
| 5-10  | 1.561           | 1.549 | -12  | 1.558 | -3                   | 1.551                               | +10 |
| 6-7   | 1.534           | 1.531 | -3   | 1.529 | -5                   | 1.533                               | +1  |
| 7-8   | 1.554           | 1.549 | -5   | 1.554 | 0                    | 1.551                               | +3  |
| 8-9   | 1.565           | 1.563 | -2   | 1.561 | -4                   | 1.565                               | 0   |
| 8-14  | 1.562           | 1.567 | +5   | 1.563 | +1                   | 1.557                               | +5  |
| 9-10  | 1.566           | 1.573 | +7   | 1.552 | -14                  | 1.561                               | +5  |
| 9-11  | 1.545           | 1.546 | +1   | 1.547 | +2                   | 1.551                               | -6  |
| 11-12 | 1.517           | 1.535 | +18  | 1.529 | +12                  | 1.517                               | 0   |
| 12-13 | 1.533           | 1.545 | +12  | 1.554 | +21                  | 1.538                               | -5  |
| 13-14 | 1.572           | 1.564 | -8   | 1.558 | -14                  |                                     |     |
| 13-18 | 1.561           | 1.569 | +8   | 1.562 | +1                   |                                     |     |
| 14-15 | 1.541           | 1.539 | -2   | 1.550 | +9                   | 1.542                               | -1  |
| 15-16 | 1.525           | 1.531 | +6   | 1.523 | -2                   | 1.526                               | -1  |
| 16-17 | 1.553           | 1.546 | -7   | 1.545 | -8                   | 1.551                               | +2  |
| 17-18 | 1.576           | 1.563 | -13  | 1.558 | -18                  |                                     |     |
| 17-22 | 1.544           | 1.539 | -5   | 1.542 | -2                   |                                     |     |
| 18-19 | 1.565           | 1.558 | -7   | 1.556 | -9                   |                                     |     |
| 19-20 | 1.567           | 1.551 | -16  | 1.538 | -29                  |                                     |     |
| 20-21 | 1.520           | 1.533 | +13  | 1.532 | +12                  |                                     |     |
| 21-22 | 1.517           | 1.529 | +12  | 1.526 | +9                   |                                     |     |
| 4-29  | 1.526           | 1.535 | +9   | 1.526 | 0                    | 1.522                               | +4  |
| 4-30  | 1.532           | 1.539 | +7   | 1.539 | +7                   | 1.531                               | +1  |
| 9-28  | 1.545           | 1.548 | +3   | 1.550 | +5                   | 1.561                               | -16 |
| 13-26 | 1.543           | 1.543 | 0    | 1.540 | -3                   |                                     |     |
| 14-27 | 1.539           | 1.551 | +12  | 1.547 | +8                   |                                     |     |
| 17-25 | 1.544           | 1.542 | -2   | 1.560 | +16                  |                                     |     |
| 20-23 | 1.540           | 1.536 | -4   | 1.556 | +16                  |                                     |     |
| 20-24 | 1.535           | 1.535 | 0    | 1.537 | +2                   |                                     |     |

$$r = \left( \frac{1}{n} \sum_{i=1}^n d_i^2 \right)^{1/2}$$

$d(CA_{calc} - CA_{obs})$  for all 36 bonds

|      |         |        |        |
|------|---------|--------|--------|
| B/M  | +0.0004 | 0.0072 | 0.0090 |
| EL/F | -0.0001 | 0.0075 | 0.0100 |

$d(CA_{calc} - CA_{obs})$  for 23 corresponding bonds

|      |         |        |        |
|------|---------|--------|--------|
| B/M  | +0.0011 | 0.0069 | 0.0089 |
| EL/F | +0.0003 | 0.0057 | 0.0077 |

$d(CA_{obs} - BO_{obs})$  for 23 corresponding bonds

|  |         |        |        |
|--|---------|--------|--------|
|  | +0.0003 | 0.0044 | 0.0063 |
|--|---------|--------|--------|

responding bond lengths with a larger r.m.s. deviation of 0.013 Å from observed values. The overall agreement between corresponding bond lengths of campanulin and baccharis oxide is significantly better than between either of the calculated/observed campanulin structure pairs.

The match between experimental and calculated valency angles (Table 3) is slightly better with B/M; the r.m.s. deviation is 1.11 vs 1.28° with EL/F. Both force fields have difficulties reproducing some of the angles involving quaternary atoms C(9) and C(10), viz 7-8-9, 8-9-10, O-10-1, O-10-9 and 1-10-9. This may, in part at least, be ascribed to the proximity of the O atom for which the FF parametrization is less

reliable, but see also discussion below on torsion angles. Calculated angles 16-17-25 and 18-17-25 differ by 1.7-2.0° from observed values; the average dis-

Table 3. Observed and calculated valency angles (°)

Calculated values under the entries B/M and EL/F are from the present work and after Faber (1977), respectively. Experimental values of some relevant valency angles in baccharis oxide (Mo, 1973) are included.

|          | Campanulin (CA) |       |      |       | Baccharis oxide (BO) | $10 \times (CA_{obs} - BO_{obs})$ |     |
|----------|-----------------|-------|------|-------|----------------------|-----------------------------------|-----|
|          | B/M             |       | EL/F |       |                      |                                   |     |
|          | obs.            | calc. | obs. | calc. |                      |                                   |     |
| 3-O-10   | 97.1            | 97.7  | +6   | 98.9  | +18                  | 97.0                              | +1  |
| 2-1-10   | 101.7           | 102.5 | +8   | 102.5 | +8                   | 102.4                             | -7  |
| 1-2-3    | 101.7           | 101.4 | -3   | 101.8 | +1                   | 101.3                             | +4  |
| O-3-2    | 102.4           | 101.3 | -11  | 101.4 | -10                  | 102.5                             | -1  |
| O-3-4    | 102.3           | 101.8 | -5   | 101.6 | -7                   | 101.8                             | +5  |
| 2-3-4    | 112.0           | 113.0 | +10  | 113.0 | +10                  | 113.6                             | -16 |
| 3-4-5    | 98.9            | 99.6  | +7   | 98.9  | 0                    | 98.8                              | +1  |
| 3-4-29   | 114.9           | 114.0 | -9   | 115.2 | +3                   | 115.4                             | -5  |
| 3-4-30   | 107.9           | 108.7 | +8   | 109.1 | +12                  | 108.6                             | -7  |
| 5-4-29   | 112.2           | 112.0 | -2   | 112.7 | +5                   | 112.6                             | -4  |
| 5-4-30   | 113.4           | 114.1 | +7   | 113.3 | -1                   | 113.5                             | -1  |
| 29-4-30  | 109.2           | 108.3 | -9   | 107.6 | -16                  | 107.8                             | +14 |
| 4-5-6    | 117.5           | 116.0 | -15  | 116.3 | -12                  | 116.7                             | +8  |
| 4-5-10   | 102.9           | 103.7 | +8   | 103.9 | +10                  | 103.4                             | -5  |
| 6-5-10   | 113.5           | 113.8 | +3   | 115.2 | +17                  | 113.5                             | 0   |
| 5-6-7    | 111.0           | 111.3 | +3   | 111.1 | +1                   | 110.6                             | +4  |
| 6-7-8    | 114.1           | 114.1 | 0    | 114.3 | +2                   | 114.4                             | -3  |
| 7-8-9    | 111.1           | 112.4 | +13  | 113.1 | +20                  | 112.2                             | -11 |
| 7-8-14   | 113.0           | 113.6 | +6   | 114.3 | +13                  | 112.3                             | +7  |
| 9-8-14   | 116.4           | 116.6 | +2   | 117.5 | +11                  | 116.6                             | -2  |
| 8-9-10   | 104.3           | 107.6 | +33  | 107.5 | +32                  | 105.5                             | -12 |
| 8-9-11   | 110.8           | 110.5 | -3   | 110.4 | -4                   | 109.6                             | +12 |
| 8-9-28   | 113.4           | 112.3 | -11  | 111.9 | -15                  | 113.9                             | -5  |
| 10-9-11  | 111.6           | 111.1 | -5   | 111.8 | +2                   | 111.9                             | -3  |
| 10-9-28  | 110.4           | 109.4 | -10  | 110.2 | -2                   | 109.7                             | +7  |
| 11-9-28  | 106.4           | 105.9 | -5   | 105.1 | -13                  | 106.4                             | 0   |
| O-10-1   | 100.7           | 99.1  | -16  | 98.5  | -22                  | 100.1                             | +6  |
| O-10-5   | 103.2           | 102.7 | -5   | 102.0 | -12                  | 102.2                             | +10 |
| O-10-9   | 111.4           | 115.6 | +42  | 115.7 | +43                  | 111.5                             | -1  |
| 1-10-5   | 105.3           | 106.2 | +9   | 105.5 | +2                   | 106.4                             | -11 |
| 1-10-9   | 119.5           | 117.2 | -23  | 118.7 | -8                   | 119.0                             | +5  |
| 5-10-9   | 114.7           | 114.0 | -7   | 114.1 | -6                   | 115.4                             | -7  |
| 9-11-12  | 114.7           | 115.1 | +4   | 115.5 | +8                   | 114.7                             | 0   |
| 11-12-13 | 112.3           | 112.5 | +2   | 112.2 | -1                   | 111.6                             | +7  |
| 12-13-14 | 106.7           | 106.9 | +2   | 106.1 | -6                   |                                   |     |
| 12-13-18 | 109.7           | 110.8 | +11  | 110.9 | +12                  |                                   |     |
| 12-13-26 | 107.8           | 106.9 | -9   | 107.2 | -6                   |                                   |     |
| 14-13-18 | 110.2           | 110.7 | +5   | 110.7 | +5                   |                                   |     |
| 14-13-26 | 111.6           | 111.8 | +2   | 112.9 | +13                  |                                   |     |
| 18-13-26 | 110.8           | 109.7 | -11  | 108.9 | -19                  |                                   |     |
| 8-14-13  | 110.2           | 110.8 | +6   | 111.1 | +9                   |                                   |     |
| 8-14-15  | 110.0           | 110.2 | +2   | 109.9 | -1                   |                                   |     |
| 8-14-27  | 110.7           | 109.8 | -9   | 109.5 | -12                  |                                   |     |
| 13-14-15 | 106.8           | 106.8 | 0    | 106.6 | -2                   | 106.4                             | +4  |
| 13-14-27 | 112.1           | 112.4 | +3   | 113.3 | +12                  |                                   |     |
| 15-14-27 | 107.0           | 106.7 | -3   | 106.3 | -7                   |                                   |     |
| 14-15-16 | 112.0           | 112.5 | +5   | 112.3 | +3                   | 112.7                             | -7  |
| 15-16-17 | 116.7           | 116.3 | -4   | 116.7 | 0                    | 117.0                             | -3  |
| 16-17-18 | 114.3           | 114.4 | +1   | 114.6 | +3                   |                                   |     |
| 16-17-22 | 108.0           | 108.5 | +5   | 109.0 | +10                  |                                   |     |
| 16-17-25 | 107.2           | 105.5 | -17  | 105.3 | -19                  |                                   |     |
| 18-17-22 | 112.1           | 111.9 | -2   | 112.3 | +2                   |                                   |     |
| 18-17-25 | 106.4           | 108.3 | +19  | 108.2 | +18                  |                                   |     |
| 22-17-25 | 108.6           | 107.9 | -7   | 107.0 | -16                  |                                   |     |
| 13-18-17 | 116.9           | 117.1 | +2   | 117.4 | +5                   |                                   |     |
| 13-18-19 | 116.3           | 116.4 | +1   | 117.8 | +15                  |                                   |     |
| 17-18-19 | 111.0           | 112.2 | +12  | 111.6 | +6                   |                                   |     |
| 18-19-20 | 122.2           | 120.2 | -20  | 120.6 | -16                  |                                   |     |
| 19-20-21 | 110.9           | 112.1 | +12  | 111.6 | +7                   |                                   |     |
| 19-20-23 | 106.4           | 107.5 | +11  | 107.5 | +11                  |                                   |     |
| 19-20-24 | 113.7           | 113.3 | -4   | 114.5 | +8                   |                                   |     |
| 21-20-23 | 109.6           | 108.0 | -16  | 108.0 | -16                  |                                   |     |
| 21-20-24 | 108.4           | 109.5 | +11  | 109.9 | +15                  |                                   |     |
| 23-20-24 | 107.6           | 106.2 | -14  | 105.0 | -26                  |                                   |     |
| 20-21-22 | 114.4           | 113.2 | -12  | 112.8 | -16                  |                                   |     |
| 21-22-17 | 113.9           | 113.1 | -8   | 113.5 | -4                   |                                   |     |

Table 3 (cont.)

|  | $\bar{\Delta}$ | $ \bar{\Delta} $ | $r = \left( \frac{1}{n} \sum_{i=1}^n \Delta_i^2 \right)^{1/2}$ |
|--|----------------|------------------|--|
| $\Delta(CA_{\text{calc}} - CA_{\text{obs}})$ for all 66 angles           |                |                  |  |
| B/M  | +0.02          | 0.84             | 1.11   |
| EL/F   | +0.12          | 1.01             | 1.28   |
| $\Delta(CA_{\text{calc}} - CA_{\text{obs}})$ for 37 corresponding angles |                |                  |  |
| B/M  | +0.09          | 0.86             | 1.20   |
| EL/F   | +0.24          | 0.95             | 1.32   |
| $\Delta(CA_{\text{obs}} - BO_{\text{obs}})$ for 37 corresponding angles  |                |                  |  |
|  | -0.04          | 0.56             | 0.69   |

crepancy for valency angles in the highly strained *E* ring is about  $1.1^\circ$  with both force fields. Again, the consistency in pairs of observed valency angles in the common structure fragment of campanulin and baccharis oxide is significantly better, average and r.m.s. deviations being reduced by about 40% relative to values for the structure produced by B/M. The results show that perturbations of bond angles (and bond lengths) caused by differences in the crystalline environment of the observed structures are relatively small and the limiting factors in the calculations of geometry must be associated mainly with the force fields.

Torsion angles are the parameters most easily influenced by packing forces. As seen in Table 4, EL/F gives values in slightly better overall agreement with observations than does B/M. Both calculated structures exhibit discrepancies comparable to or smaller than those between the observed structures. Prediction of torsion angles for the atomic sequence 8–9–10–5 of ring *B* is inadequate with either force field. The largest differences between baccharis oxide and campanulin also occur in this ring. In fact, we observe that about 25% of the intermolecular contacts within limits given previously (Mo, 1977) involve atoms of the groups C(6)H<sub>2</sub>, C(7)H<sub>2</sub> and C(8)H, another 25% involve C(12)H<sub>2</sub> and methyl C(28)H<sub>3</sub>, the latter being attached to C(9). It is conceivable that these local changes in the campanulin crystal relative to baccharis oxide (Mo, 1973) contribute to the increased dif-

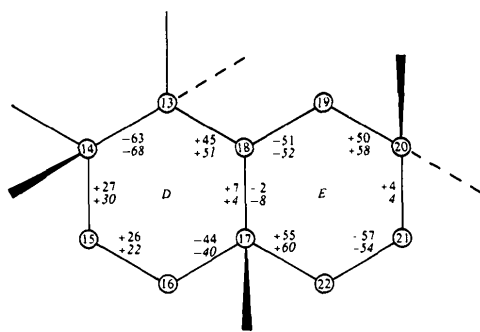


Fig. 2. Calculated torsion angles ( $^\circ$ ) in rings *D* and *E* of the campanulin *S* form. Numbers in italics are the observed values in  $3\beta$ -friedelanol (Laing *et al.*, 1977).

Table 4. Observed and calculated torsion angles ( $^\circ$ )

Calculated values under the entries B/M and EL/F are from the present work and after Faber (1977), respectively. Experimental values of some relevant torsion angles in baccharis oxide (Mo, 1973) are included.

|  | Campanulin (CA) |       |                       |       |                       |             |  |  |
|--|-----------------|-------|-----------------------|-------|-----------------------|-------------|--|--|
|  | B/M             |       | EL/F                  |       | Baccharis oxide       |             | 10 ×   |  |
|  | obs.            | calc. | 10 × (calc.) - (obs.) | calc. | 10 × (calc.) - (obs.) | (BO) (obs.) | 10 × (CA <sub>obs</sub> ) - (BO <sub>obs</sub> )               |  |
| Ring <i>a</i>                          |                 |       |                       |       |                       |             |  |  |
| 1,2                                    | +3.1            | +2.2  | -9                    | +3.8  | +7                    | +1.6        | +15  |  |
| 2,3                                    | +32.1           | +33.2 | +11                   | +31.1 | -10                   | +33.6       | -15  |  |
| 3,0                                    | -56.2           | -58.1 | +19                   | -57.0 | +8                    | -57.2       | -10  |  |
| O,10                                   | +57.7           | +58.4 | +7                    | +58.2 | +5                    | +57.0       | +7   |  |
| 10,1                                   | -37.0           | -36.5 | -5                    | -37.2 | +2                    | -35.7       | +13  |  |
| Ring <i>b</i>                          |                 |       |                       |       |                       |             |  |  |
| 4,5                                    | +11.1           | +10.3 | -8                    | +12.1 | +10                   | +9.7        | +14  |  |
| 5,10                                   | +23.8           | +24.2 | +4                    | +22.2 | -16                   | +25.5       | -17  |  |
| 10,0                                   | -51.0           | -50.6 | -4                    | -49.8 | -12                   | -52.4       | -14  |  |
| O,3                                    | +59.9           | +58.7 | -12                   | +59.7 | -2                    | +60.5       | -6   |  |
| 3,4                                    | -43.5           | -42.1 | -14                   | -43.2 | -3                    | -42.8       | +7   |  |
| Ring <i>A</i>                          |                 |       |                       |       |                       |             |  |  |
| 1,2                                    | +3.1            | +2.2  | -9                    | +3.8  | +7                    | +1.6        | +15  |  |
| 2,3                                    | -76.8           | -74.9 | -19                   | -76.9 | +1                    | -75.5       | +13  |  |
| 3,4                                    | +65.4           | +65.7 | +3                    | +64.7 | -7                    | +66.7       | -13  |  |
| 4,5                                    | +11.1           | +10.3 | -8                    | +12.1 | +10                   | +9.7        | +14  |  |
| 5,10                                   | -81.4           | -79.3 | -21                   | -80.3 | -11                   | -79.0       | +24  |  |
| 10,1                                   | +70.0           | +69.6 | -4                    | +67.9 | -21                   | +70.3       | -3   |  |
| Ring <i>B</i>                          |                 |       |                       |       |                       |             |  |  |
| 5,6                                    | -56.1           | -58.0 | +19                   | -55.8 | -3                    | -57.2       | -11  |  |
| 6,7                                    | +31.0           | +29.9 | -11                   | +31.2 | +2                    | +32.5       | -15  |  |
| 7,8                                    | +30.9           | +29.7 | -12                   | +26.7 | -42                   | +28.0       | +29  |  |
| 8,9                                    | -67.1           | -62.8 | -43                   | -61.7 | -54                   | -63.5       | +36  |  |
| 9,10                                   | +42.2           | +34.9 | -73                   | +37.5 | -47                   | +39.1       | +31  |  |
| 10,5                                   | +17.2           | +23.1 | +59                   | +19.3 | +21                   | +19.2       | -20  |  |
| Ring <i>C</i>                          |                 |       |                       |       |                       |             |  |  |
| 8,9                                    | +41.3           | +42.1 | +8                    | +39.5 | -18                   | +44.2       | -29  |  |
| 9,11                                   | -43.4           | +43.5 | +1                    | -41.7 | -17                   | -46.5       | -31  |  |
| 11,12                                  | +57.5           | +56.2 | -13                   | +56.4 | -11                   | +57.6       | -1   |  |
| 12,13                                  | -63.5           | -61.5 | -20                   | -62.7 | -8                    | -61.5       | +20  |  |
| 13,14                                  | +58.9           | +58.2 | -7                    | +58.5 | -4                    | +57.3       | +16  |  |
| 14,8                                   | -50.7           | -51.5 | +8                    | -50.3 | -4                    | -51.3       | -6   |  |
| Ring <i>D</i>                          |                 |       |                       |       |                       |             |  |  |
| 13,14                                  | -62.5           | -61.0 | -15                   | -61.4 | -11                   | -61.4       | -11  |  |
| 14,15                                  | +64.9           | +64.0 | -9                    | +64.2 | -7                    | +64.2       | -7   |  |
| 15,16                                  | -49.4           | -50.0 | +6                    | -49.0 | -4                    | -49.0       | -4   |  |
| 16,17                                  | +29.8           | +31.1 | +13                   | +29.3 | -5                    | +29.3       | -5   |  |
| 17,18                                  | -29.0           | -29.9 | +9                    | -28.1 | -9                    | -28.1       | -9   |  |
| 18,13                                  | +46.2           | +46.0 | -2                    | +45.4 | -8                    | +45.4       | -8   |  |
| Ring <i>E</i>                          |                 |       |                       |       |                       |             |  |  |
| 17,18                                  | -42.3           | -44.4 | +21                   | -43.5 | +12                   | -43.5       | +12  |  |
| 18,19                                  | +34.6           | +36.6 | +20                   | +37.9 | +33                   | +37.9       | +33  |  |
| 19,20                                  | -35.2           | -37.0 | +18                   | -39.4 | +42                   | -39.4       | +42  |  |
| 20,21                                  | +44.4           | +45.7 | +13                   | +47.0 | +26                   | +47.0       | +26  |  |
| 21,22                                  | -58.0           | -57.8 | -2                    | -57.3 | -7                    | -57.3       | -7   |  |
| 22,17                                  | +56.0           | +56.6 | +6                    | +55.3 | -7                    | +55.3       | -7   |  |
|  |                 |       | $\bar{\Delta}$        |       | $ \bar{\Delta} $      |             | $r = \left( \frac{1}{n} \sum_{i=1}^n \Delta_i^2 \right)^{1/2}$ |  |
| Ring <i>a</i>                          |                 |       |                       |       |                       |             |  |  |
| CA <sub>calc</sub> - CA <sub>obs</sub> | B/M             | +0.46 | 1.02                  | 1.13  |                       |             |  |  |
| CA <sub>obs</sub> - BO <sub>obs</sub>  | EL/F            | +0.24 | 0.64                  | 0.70  |                       |             |  |  |
|  |                 | +0.20 | 1.20                  | 1.24  |                       |             |  |  |
| Ring <i>b</i>                          |                 |       |                       |       |                       |             |  |  |
| CA <sub>calc</sub> - CA <sub>obs</sub> | B/M             | -0.68 | 0.84                  | 0.93  |                       |             |  |  |
| CA <sub>obs</sub> - BO <sub>obs</sub>  | EL/F            | -0.46 | 0.86                  | 1.01  |                       |             |  |  |
|  |                 | -0.32 | 1.16                  | 1.24  |                       |             |  |  |
| Ring <i>A</i>                          |                 |       |                       |       |                       |             |  |  |
| CA <sub>calc</sub> - CA <sub>obs</sub> | B/M             | -0.97 | 1.07                  | 1.27  |                       |             |  |  |
| CA <sub>obs</sub> - BO <sub>obs</sub>  | EL/F            | -0.35 | 0.95                  | 1.13  |                       |             |  |  |
|  |                 | +0.83 | 1.37                  | 1.50  |                       |             |  |  |
| Ring <i>B</i>                          |                 |       |                       |       |                       |             |  |  |
| CA <sub>calc</sub> - CA <sub>obs</sub> | B/M             | -1.02 | 3.62                  | 4.34  |                       |             |  |  |
| CA <sub>obs</sub> - BO <sub>obs</sub>  | EL/F            | -2.05 | 2.82                  | 3.50  |                       |             |  |  |
|  |                 | +0.83 | 2.37                  | 2.53  |                       |             |  |  |

Table 4 (cont.)

|  |      | $\bar{d}$ | $ \bar{d} $ | $r = \left( \frac{1}{n} \sum_{i=1}^n d_i^2 \right)^{1/2}$ |
|--|------|-----------|-------------|---|
| Ring C                                 |      |           |             |   |
| CA <sub>calc</sub> - CA <sub>obs</sub> | B/M  | -0.38     | 0.95        | 1.12  |
|  | EL/F | -1.03     | 1.03        | 1.18  |
| CA <sub>obs</sub> - BO <sub>obs</sub>  |      | -0.52     | 1.72        | 2.04  |
| Ring D                                 |      |           |             |   |
| CA <sub>calc</sub> - CA <sub>obs</sub> | B/M  | +0.03     | 0.90        | 0.97  |
|  | EL/F | -0.73     | 0.73        | 0.77  |
| Ring E                                 |      |           |             |   |
| CA <sub>calc</sub> - CA <sub>obs</sub> | B/M  | +1.27     | 1.33        | 1.51  |
|  | EL/F | +1.65     | 2.12        | 2.51  |

ferences in torsion angles and, possibly, also valency angles in or near ring *B*.

Field B/M calculates the *F* form of campanulin to be the more stable by 7.7 kJ mol<sup>-1</sup> (1.85 kcal mol<sup>-1</sup>). EL/F also favours this form relative to *S* with an energy difference of 12.4 kJ mol<sup>-1</sup> (2.95 kcal mol<sup>-1</sup>). This is a satisfactory agreement.

Calculated torsion angles for rings *D* and *E* of the *S* form are displayed in Fig. 2 together with the values reported for structure (IV*b*) at a crystallographic *R* = 0.17 (Laing *et al.*, 1977).

### Conclusions

Conformational studies of the pentacyclic triterpene campanulin by two different force fields, basically those of Boyd (present study) and Ermer & Lifson (Faber, 1977), have given structure parameters in generally good agreement with values obtained from a crystallographic study. The results corroborate the assumption that the X-ray structure is essentially determined by intramolecular forces and strengthen the view that FF methods are capable of yielding quite accurately the geometry of strained ring systems of such complexity.

The largest discrepancies with observed torsion angles appear in ring *B* which is true also when the X-ray structures of campanulin and the closely related baccharis oxide are compared. A larger number of intermolecular contacts involving atoms in this region of campanulin and the proximity of an ether O atom are factors that probably contribute to the systematic deviations.

With few exceptions, mainly in some bond lengths, the trend in calculated structure parameters shown by the two force fields is remarkably similar. This is a particularly gratifying result in view of the differences in parametrization and complexity.

Both force fields favour the *F* form of campanulin, a result which is not at all obvious from inspection of rigid Dreiding models but is consistent with the X-ray study. The calculated energy difference between the *F* and *S* forms is only ~8–12.5 kJ mol<sup>-1</sup> (~2–3 kcal mol<sup>-1</sup>). This is comparable to or slightly larger than differences in lattice energy for crystalline polymorphs (Kitaigorodsky, 1970; Brock & Ibers, 1976). If the barrier separating the two forms is of similar mag-

nitude, the order of preference could easily be reversed with a change in substitution.

Similar considerations apply to the related friedelane system. In this context it is an intriguing observation that 3β-friedelanol is *S* while the chloroacetate of the α-epimer appears to be *F*. Changes in the crystalline environment and in the long-range transmission of intramolecular strain due to different substituents could be responsible for the change of conformation. These points will be further explored in a combined X-ray and FF study of friedelin now in progress.

The author thanks Drs J. Krane and R. E. Stølevik and Professor H. Sørum for valuable discussions, the former also for kindly making the program *MOLBD2* available. He is also indebted to Drs D. H. Faber and M. Laing for providing unpublished results. Mr K. R. Holm is thanked for advice during the implementation of a modified version of this program on the local Univac 1100/21 computer.

### References

- ALTONA, C. & FABER, D. H. (1974). *Top. Curr. Chem.* **45**, 1–38.
- BOYD, R. H. (1968). *J. Chem. Phys.* **49**, 2574–2583.
- BOYD, R. H. (1975). *J. Am. Chem. Soc.* **97**, 5353–5357.
- BOYD, R. H., BREITLING, S. M. & MANSFIELD, M. (1973). *Am. Inst. Chem. Eng. J.* **19**, 1016–1024.
- BROCK, C. P. & IBERS, J. A. (1976). *Acta Cryst.* **A32**, 38–42.
- CHANG, S., MCNALLY, D., SHARY-TEHRANY, S., HICKEY, M. J. & BOYD, R. H. (1970). *J. Am. Chem. Soc.* **92**, 3109–3118.
- COREY, E. J. & URSPRUNG, J. J. (1956). *J. Am. Chem. Soc.* **78**, 5041–5051.
- DUNITZ, J. D. & BÜRGI, H. B. (1975). *MTP International Review of Science: Physical Chemistry*, Series 2. Vol. 11, edited by J. M. ROBERTSON, pp. 81–120. London and Boston: Butterworths.
- ENGLER, E. M., ANDOSE, J. D. & SCHLEYER, P. VON R. (1973). *J. Am. Chem. Soc.* **95**, 8005–8025.
- ERMER, O. (1976). *Struct. Bonding (Berlin)*, **27**, 161–211.
- ERMER, O. & LIFSON, S. (1973). *J. Am. Chem. Soc.* **95**, 4121–4132.
- FABER, D. H. (1977). Private communication (forthcoming thesis).
- KITAIGORODSKY, A. I. (1970). *Adv. Struct. Res. Diffraction Methods*, **3**, 225.
- LAING, M., BURKE-LAING, M. E., BARTHO, R. & WEEKS, C. M. (1977). *Tetrahedron Lett.* pp. 3839–3842.
- MASAKI, N., NIWA, M. & KIKUCHI, T. (1975). *J. Chem. Soc. Perkin Trans. 2*, pp. 610–614.
- MO, F. (1973). *Acta Cryst.* **B29**, 1796–1807.
- MO, F. (1977). *Acta Cryst.* **B33**, 641–649.
- ROGERS, D., WILLIAMS, D. J., JOSHI, B. S., KAMAT, V. N. & VISWANATHAN, N. (1974). *Tetrahedron Lett.* pp. 63–66.
- ROMERS, C., ALTONA, C., JACOBS, H. J. C. & DE GRAAFF, R. A. G. (1974). *Chem. Soc. Spec. Period. Rep.* **4**, 531–583.
- WHITE, D. N. J. & BOVILL, M. J. (1977). *J. Chem. Soc. Perkin Trans. 2*, pp. 1610–1623.